Chemical Geology 282 (2011) 113–119

Contents lists available at ScienceDirect

Chemical Geology

journal homepage: www.elsevier.com/locate/chemgeo

Research paper

A mass-balance model to separate and quantify colloidal and solute redistributions in soil

Carleton R. Bern [a,*], Oliver A. Chadwick [b], Anthony S. Hartshorn [c], Lesego M. Khomo [d], Jon Chorover [e]

[a] U.S. Geological Survey, Denver Federal Center, Denver, CO 80225–0046, United States
[b] Department of Geography, University of California, Santa Barbara, CA 93106–4060, United States
[c] Dept. of Geology and Environmental Science, James Madison University, Harrisonburg, VA 22807, United States
[d] Animal, Plant, and Environmental Sciences, University of the Witwatersrand, Johannesburg 2050, South Africa
[e] Dept. of Soil, Water and Environmental Science, University of Arizona, Tucson, AZ 85721, United States

ARTICLE INFO

Article history:
Received 12 April 2010
Received in revised form 14 January 2011
Accepted 23 January 2011
Available online 28 January 2011

Editor: J.D. Blum

Keywords:
Kruger National Park
Index element
Mass-balance
Mixing equation
Soil
Weathering

ABSTRACT

Studies of weathering and pedogenesis have long used calculations based upon low solubility index elements to determine mass gains and losses in open systems. One of the questions currently unanswered in these settings is the degree to which mass is transferred in solution (solutes) versus suspension (colloids). Here we show that differential mobility of the low solubility, high field strength (HFS) elements Ti and Zr can trace colloidal redistribution, and we present a model for distinguishing between mass transfer in suspension and solution. The model is tested on a well-differentiated granitic catena located in Kruger National Park, South Africa. Ti and Zr ratios from parent material, soil and colloidal material are substituted into a mixing equation to quantify colloidal movement. The results show zones of both colloid removal and augmentation along the catena. Colloidal losses of 110 kg m^{-2} (−5% relative to parent material) are calculated for one eluviated soil profile. A downslope illuviated profile has gained 169 kg m^{-2} (10%) colloidal material. Elemental losses by mobilization in true solution are ubiquitous across the catena, even in zones of colloidal accumulation, and range from 1418 kg m^{-2} (−46%) for an eluviated profile to 195 kg m^{-2} (−23%) at the bottom of the catena. Quantification of simultaneous mass transfers in solution and suspension provide greater specificity on processes within soils and across hillslopes. Additionally, because colloids include both HFS and other elements, the ability to quantify their redistribution has implications for standard calculations of soil mass balances using such index elements.

Published by Elsevier B.V.

1. Introduction

Catenas are hydrologically linked hillslope soils that lose or gain dissolved and particulate soil constituents depending on topographic position (Huggett, 1975; Sommer and Schlichting, 1997). In gently sloping landscapes where physical erosion rates are low and where soil contains abundant coarse particles, mass redistribution can occur as subsurface flow of dissolved and/or colloidal material (plasma) through a relatively immobile skeleton of the coarser grained particles (Jenny and Smith, 1935). Similar to vertical transfers down individual soil profiles, these mass losses and gains produce eluvial and illuvial zones, respectively. Eluvial and illuvial zones are prominent features of soils and are indicative of fundamental transport processes. Colloidal transport is often assumed to be important when aluminosilicate clays and metal oxyhydroxides accumulate in soil, and yet—compared with solution processes—we understand relatively little about many of fundamental processes associated with mobilization, transport and immobilization of colloids (McCarthy and McKay, 2004).

Various aspects of soil colloid mobilization have been clarified through laboratory studies using packed columns or intact soil monoliths (Jenny and Smith, 1935; Laegdsmand et al., 1999). For instance, colloidal mobilization (dispersion) is strongly influenced by parameters that affect electrostatic repulsion via the magnitude and sign of particle surface charge; these include the pH, ionic strength, and ionic composition of the soil solution (Bunn et al., 2002; Heil and Sposito, 1993; Suarez et al., 1984). Colloid mobilization has also been linked to commonly occurring fluctuations of soil iron redox status via rapid and substantial pH shifts (Thompson et al., 2006). By contrast, our understanding of the complexity and magnitudes of *in-situ* colloid mobilization, transport, and retention is less extensive (McCarthy and McKay, 2004). Movement of suspended colloidal material is a primary means of mobilizing low-solubility and sorptive components (Kretzschmar et al., 1999). Recalcitrant, high field strength (HFS) elements like Ti, and to a lesser extent Zr, exhibit mobility in soil (Colin et al., 1993; Cornu et al., 1999; Kurtz et al., 2000). That mobility has been linked to transport via colloids (Thompson et al., 2006), raising questions regarding the extent to which such elements truly

* Corresponding author. Tel.: +1 303 236 1024; fax: +1 303 236 3200.
E-mail addresses: cbern@usgs.gov (C.R. Bern), oac@geog.ucsb.edu (O.A. Chadwick), hartshas@jmu.edu (A.S. Hartshorn), lesegok@gmail.com (L.M. Khomo), chorover@cals.arizona.edu (J. Chorover).

0009-2541/$ – see front matter. Published by Elsevier B.V.
doi:10.1016/j.chemgeo.2011.01.014

serve as immobile indices against which to measure the gains and losses of other elements in bulk soil (Brewer, 1964; Brimhall and Dietrich, 1987). Colloidal material has also been noted as a potentially significant means of redistributing elements like Fe and Mg that are more commonly assumed to move in solution (Gasser et al., 1994). There have been some *in-situ* studies of colloidal soil fluxes over time scales of hours and days (Ryan et al., 1998). However, longer-term colloidal transfers have been only implicitly evaluated within soil profiles (Brewer, 1964; Walker and Chittleborough, 1986) and along hydrologically connected hillslopes (Paton et al., 1995) while quantification of such fluxes has remained elusive.

Here we provide a model for quantifying the long-term effect of through-soil colloidal transfers using Ti and Zr as tracers and apply it to a granitic catena in southern Africa. This model distinguishes between mass redistribution via colloids versus solution and provides a comparison of the effectiveness of those processes *in situ* and over the time-scale of soil formation.

2. Methods

Horizons from ten soil profiles were sampled along a 150-m catena (Fig. 1) developed on gently rolling hills underlain by Archaean granite and gneiss of the Nelspruit suite (Barton et al., 1986) and adjacent to the SAFARI-2000 flux tower in Kruger National Park, South Africa (Scholes et al., 2001). The granitic parent material creates a sandy, quartz-rich soil skeleton through which dissolved and suspended material can flow; the parent material combines with low erosion rates and sufficient rainfall to form unusually well-differentiated catenas (Khomo, 2008; Venter, 1986). The catena was separated into three zones: a clay-poor upslope position, a clay-poor seepline position, and a clay-rich downslope position (Fig. 1). The seepline is a narrow zone, just upslope of the clay-rich zone, where subsurface water is forced to the surface during high flow by the low conductivity clays downslope. The seepline soils are highly leached, whitish soils that have been mostly stripped of iron and clays due to fluctuating redox conditions (Venter, 1986).

Samples from sixty-five soil horizons were air-dried, sieved to <2 mm, and ground to powder. Hand samples of local rock types were collected from outcrops <2 km from the catena or from below soil saprolite. Oxidized or stained outer material was cut away and the remaining material was pulverized. Major and trace element concentrations were measured by wave-dispersive and energy-dispersive X-ray fluorescence, respectively, by ALS Chemex (Reno, Nevada). Any use of trade, product, or firm names is for descriptive purposes only and does not imply endorsement by the U.S. Government. Soil bulk density was measured using saran-coated clods (Blake and Hartge, 1986) and particle size by a modified hydrometer method (Gee and Bauder, 1986).

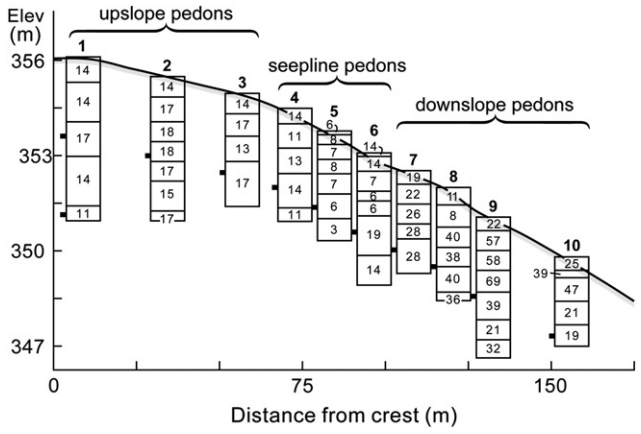

Fig. 1. Diagram of the catena showing relative profile locations, horizon thicknesses, and clay contents (%). Profile depth is exaggerated with small filled squares noting 50 cm increments.

Mean annual precipitation at a nearby weather station averages 55 cm, nearly all in the austral summer (Scholes et al., 2001). The sandier upslope and seepline soils of the catena have higher infiltration rates and average 0.7 m to C horizons. Water moves downslope through the soil until it reaches the clay-rich zone whereupon it surfaces at the seepline and runs overland across the toe of the slope. In wet years the seepline soils can remain near saturation for a month or two at the end of the November-to-March rainy season. To evaluate the concentrations of solutes and colloids being carried downslope, we collected a sample of water from a clay-poor seepline soil (profile 5) in April 2009. A fresh soil pit was hand dug to a depth of 0.8 m and cloudy water was observed seeping from large pores in the grain-supported open-matrix soil fabric. The pit was left undisturbed for five hours, and about 0.3 m of water accumulated in the bottom. Water was carefully dipped from the pond using an acid-washed plastic bottle, then promptly filtered into another plastic bottle using syringe filters with a nominal pore size of 1 μm (Pall Type A/E, Glass Fiber, P/N 61631). Numerous filters clogged during the production of a 0.8-L sample, and the filtered water remained cloudy (i.e., a stable colloidal suspension) even after five days of refrigeration. Undoubtedly this sample contained colloids entrained both naturally and as a result of sampling disturbance but such disturbance likely contributed colloids similar to those mobilized by normal bioturbation such as tree-throw and burrowing. Additionally, colloids mobilized *in situ* are understood to have compositions generally similar to the fine fractions present in soil (Kretzschmar et al., 1999).

A split of the field-filtered sample was centrifuged to remove particles >0.066 μm. A split of the resulting supernatant was then filtered using pre-rinsed, mixed-cellulose–ester membranes to remove particles >0.025 μm. The field-filtered sample was digested with HNO_3 and HF by EPA method 3502 (U.S. EPA, 1986). The centrifuged and membrane-filtered splits were acidified with HNO_3, and after a few days colloidal material was again visible in the centrifuged split, but not in the membrane-filtered split. All three splits were subjected to elemental analysis by ICP-MS at the University of Arizona. Calibration standards were prepared from stock solutions obtained from AccuStandard (New Haven, CT). Instrument detection limits were <0.1 pV/V for the elements reported. Check solutions from independent sources (e.g. NIST 1643e) were analyzed during sample runs and results fell within 25% of expected values. A split of the field-filtered sample was subsequently subjected to a four-acid digest (HNO_3, HCl, HF and $HClO_4$) and analyzed again at USGS in Denver, Colorado alongside the soil standard NIST 2709. Recoveries for Al, Fe, Ti, and Zr were 89%, 91%, 80%, and 18% for NIST 2709. Low recovery for Zr is likely due to its occurrence in zircons, which are resistant to acid dissolution. However, the large surface to mass ratio of the colloidal material in the field-filtered sample should have aided in digestion and undigested colloids may still have entered the instrument and been incorporated into the analysis. This suggests Zr recovery for the colloid sample could be higher than for the soil standard. Concentrations of Al, Fe, Ti, and Zr measured in the field-filtered sample digest at USGS were 109%, 103%, 117%, and 82% of those measured at the University of Arizona. The differences may be the result of the different digest procedures and durations. Data from the University of Arizona are presented here and used in subsequent calculations.

Total dissolved and suspended solids were determined gravimetrically on portions of the field-filtered and membrane-filtered splits after drying at 100 °C in an oven. Field-filtered water was pipetted onto a glass slide, dried, and the colloidal material was analyzed by X-ray diffraction that included glycolation and heat treatments at the USGS in Denver, Colorado. A separate split of field-filtered sample was air dried and examined using a FEI Quanta 450 FEG Scanning Electron Microscope with an EDAX Energy Dispersive Spectroscopy (EDS) instrument at the USGS in Denver, Colorado.

3. Results

3.1. Colloidal material

Dissolved plus colloidal material averaged (±1 S.D.) 9.7 ± 0.7 mg g^{-1} of the field-filtered catena water sample, and dissolved solids were 0.20 ± 0.13 mg g^{-1} of the membrane-filtered split, indicating ~9.5 mg g^{-1} total colloids. X-ray diffraction indicated the presence of smectite, halloysite, and kaolinite in the colloidal material. Element concentrations measured by ICP-MS (Table 1) accounted for 50% of dissolved and suspended solids in the field-filtered sample, with non-analyte elements (e.g. oxygen) comprising the balance. The chemistry of the membrane-filtered split (pH 6.7) was modeled in PHREEQC (Parkhurst and Appelo, 1999) which indicated oversaturation relative to several mineral phases including amorphous aluminum oxides and silica, goethite, hematite, illite, smectite, potassium mica, and kaolinite. These data suggest that the membrane-filtered split may contain such phases in nano-particulate (<0.025 μm) forms, or that their presence in the membrane filtrate is limited by slow kinetics of nucleation and crystal growth. Differences in element concentrations between the centrifuged split and membrane-filtered split suggest which elements are contained in <0.066 μm forms. Ti concentrations decrease 180-fold between the centrifuged and membrane-filtered split, demonstrating that sparingly soluble elements are strongly partitioned into these smaller colloids, while Fe and Al concentrations decrease 39- and 8-fold respectively.

Element concentrations in colloids were calculated by subtracting the dissolved (membrane-filtered) component from the field-filtered sample and dividing by gravimetric colloidal mass. Concentrations of Ti and Zr were low and below detection limits respectively in the membrane-filtered split, as expected from their low solubility. In contrast, their concentrations in the colloidal fraction were much higher, indicating potentially significant transport in suspension.

SEM examination of the dried, field-filtered sample in backscatter mode identified some high-density particles. EDS examination showed one of these particles (0.7 μm in diameter) to have high Zr content, and it was identified as zircon (Fig. 2). Several other particles roughly 0.7 μm in size had high Ti and Fe contents and were tentatively identified as ilmenite (Fig. 2).

3.2. High field strength element ratios

Ratios of HFS element concentrations (e.g. Ti/Zr) have been used to assess soil mobility of those elements (Kurtz et al., 2000). Other formulations using such pairs of concentrations have been used to infer derivation of soils from particular mixtures of parent materials (Sommer et al., 2000). We calculated a HFS element ratio as

$$R_{Ti/(Ti+Zr)} = \frac{Ti}{Ti + Zr}, \quad (1)$$

where *Ti* and *Zr* are element concentrations in mg kg^{-1}. This formulation is necessitated by calculations presented in the discussion.

Table 1
Element concentrations measured in splits of the soil water sample and calculated for colloids as described in the text. ND = not detected.

Element	Field-filtered sample (<~1 μm) (mg L^{-1})	Centrifuged split (<0.066 μm) (mg L^{-1})	Membrane-filtered split (<0.025 μm) (mg L^{-1})	Colloids (mg kg^{-1})
Al	1034 ± 1	16.9 ± 0.4	1.80 ± 0.02	110,000 ± 10,000
Fe	443 ± 4	16 ± 1	0.395 ± 0.004	46,000 ± 4000
Ti	104 ± 2	0.18 ± 0.05	0.0010 ± 0.0006	11,000 ± 1000
Zr	0.76 ± 0.07	0.0025 ± 0.0003	ND	80 ± 7

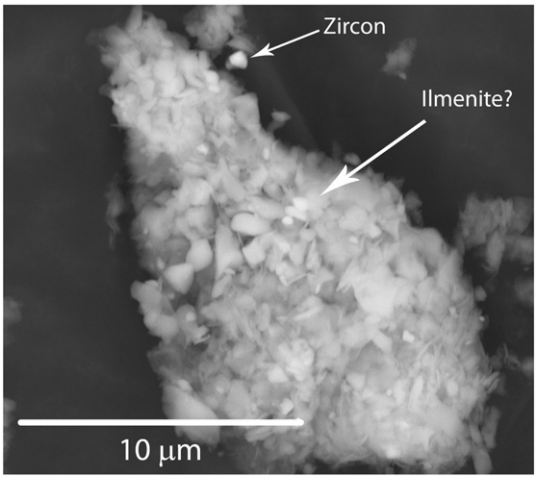

Fig. 2. Scanning electron microscope, backscattered electron image of aggregated, air dried material from the field-filtered sample. Image collected at 20 kV accelerating voltage and 10 mm working distance. High-density phases appear brighter. Ti and Zr bearing phases are identified in the figure.

$R_{Ti/(Ti+Zr)}$ changes between soil horizons as well as along the catena (Fig. 3). Upslope profiles show little variability with depth, whereas $R_{Ti/(Ti+Zr)}$ in seepline and downslope profiles shows substantial changes with depth. Some seepline and upslope horizons have $R_{Ti/(Ti+Zr)}$ values below the range determined for the presumed granitic parent material. Mafic xenoliths are present as a pervasive but volumetrically minor rock type in outcrops near the catena, but considering them as a potential subcomponent of parent material does not help explain soil $R_{Ti/(Ti+Zr)}$ patterns because these xenolith values comprise three of the four highest, not lowest, $R_{Ti/(Ti+Zr)}$ values (Fig. 3).

Clay is the soil size fraction (<2 μm) that includes colloids (<1 μm). Linear regression shows that soil horizon clay content correlates positively with Ti ($p<0.0001$, $R^2 = 0.44$, $F = 43$, $n = 58$) and negatively with Zr ($p<0.0001$, $R^2 = 0.41$, $F = 39$, $n = 58$) thus supporting the high $R_{Ti/(Ti+Zr)}$ calculated for the single sample of colloids (0.9928). Soil $R_{Ti/(Ti+Zr)}$ is correlated strongly and positively with clay ($p<0.0001$, $R^2 = 0.67$, $F = 112$, $n = 58$).

4. Discussion

4.1. Patterns of colloidal movement

The relatively small variability of $R_{Ti/(Ti+Zr)}$ in deeper soil and C horizons, argues against a systematic change in soil parent material with distance from crest, as observed on some other catenas (Sommer et al., 2000). Assuming the soils examined here have formed from granite parent material with $R_{Ti/(Ti+Zr)}$ similar to those found in the rock samples and C horizons, the vertical shifts in $R_{Ti/(Ti+Zr)}$ (Fig. 3) must result from either: 1) addition of exogenous material or 2) differential mobility of HFS elements. Exogenous dust must be considered as it would particularly influence the surface, and the low relief and low erosion rates would favor its accumulation. However, the differences in $R_{Ti/(Ti+Zr)}$ between catena sections would require substantial differences in dust accumulation rates along the relatively short and gentle slope that seem unlikely.

In contrast, our data support differential physical mobility of HFS elements. Association of Ti but not Zr with clay content indicates that clay transfers should preferentially redistribute Ti over Zr. Relatively high HFS element concentrations in the colloid sample indicate that colloids are the likely medium for redistribution. The high $R_{Ti/(Ti+Zr)}$ value of the colloid sample is consistent with the direction of ratio shifts expected if colloids were being eluviated from upslope and seepline profiles and illuviated into downslope profiles (Fig. 3). We

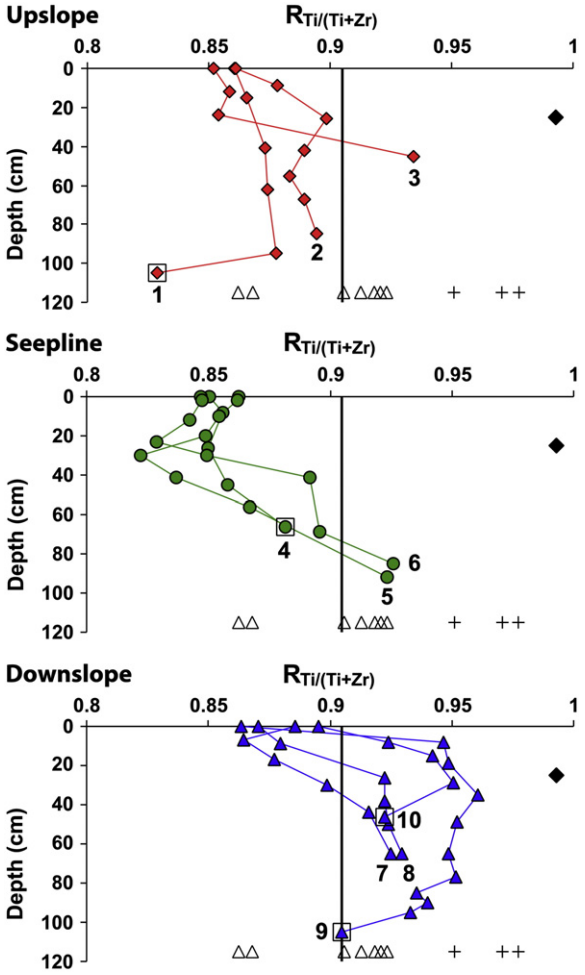

Fig. 3. Soil horizon $R_{Ti/(Ti+Zr)}$ values for the <2 mm fraction plotted by depth and separated by catena position. Data points for C or R horizons included in parent material average are designated by a surrounding box. Profile numbers are printed next to corresponding data. Colloids are represented by black diamonds plotted arbitrarily at 25 cm depth. Hand samples of granites are shaded triangles and crosses are mafic xenoliths, both plotted arbitrarily at 115 cm depth. The solid vertical line is the mean $R_{Ti/(Ti+Zr)}$ of granites and C horizons (0.9049) and separates zones of implied eluviation and illuviation.

take the $R_{Ti/(Ti+Zr)}$ calculated from the mean concentrations of Ti and Zr in all the granite and C horizon samples (0.9049, n = 12) to be a reasonable parent material value. Plotting this value as a line on Fig. 3 demarcates the boundary between colloidal eluviation and illuviation. Upslope and seepline profiles have lost colloidal material and the clay-rich B horizons of downslope profiles have gained colloidal material. These colloidal eluvial/illuvial patterns support prior notions of through-soil mass transfers along catenas (Huggett, 1975; Sommer and Schlichting, 1997), but quantification is required to assess their importance relative to other pedogenic processes.

4.2. Quantifying colloidal movement

The $R_{Ti/(Ti+Zr)}$ of colloids provides a fingerprint for visualizing colloidal redistributions in soil (Fig 2). Here we present a model for quantifying both that mass redistribution and, by difference, redistribution of mass via solution.

Two-component mixing equations have become standard tools for determining the contribution of distinct source components to a mixture by using element concentrations, element ratios, or isotope ratios as tracers (Faure, 1977). Such calculations assume that processes other than mixing do not affect the relevant tracers. We treat the redistribution of colloids as a mixing situation and assume that colloidal transfer is the only significant means of gain or loss for Ti and Zr in soil along the catena. Low (dissolved) Ti and Zr concentrations in the membrane-filtered water sample support this assumption.

The tracer applied here is the element ratio $R_{Ti/(Ti+Zr)}$, which traces the combined masses of Ti and Zr represented by

$$m = Ti + Zr. \tag{2}$$

Abbreviating $R_{Ti/(Ti+Zr)}$ to R, that ratio in a given sample of soil (S) reflects the mass contributions of two components, granitic soil parent material (PM) and colloids (C) mixed into it, by the relationship

$$R_S = \frac{R_C m_C + R_{PM} m_{PM}}{m_C + m_{PM}}. \tag{3}$$

We define the parameter upsilon (υ) as the proportion of Ti and Zr contributed to a sample of soil by the colloidal component:

$$\upsilon = \frac{m_C}{m_C + m_{PM}} \tag{4}$$

The ratio of the tracer elements in soil can then also be calculated using υ to represent the mass proportions by:

$$R_S = R_C\upsilon + R_{PM}(1-\upsilon). \tag{5}$$

From Eq. (5), the ratio of tracer elements in soil can then be understood to be a linear function of υ:

$$R_S = \upsilon(R_C - R_{PM}) + R_{PM}. \tag{6}$$

Eq. (6) in turn can be rearranged to yield a mixing equation that is also frequently used in isotopic studies:

$$\upsilon = \frac{R_S - R_{PM}}{R_C - R_{PM}}. \tag{7}$$

By substituting the $R_{Ti/(Ti+Zr)}$ of colloids, parent material and a soil sample into Eq. (7), the proportion of Ti and Zr sourced from the colloid component (υ) can be calculated.

While the relationships described above are commonly used to quantify tracer mixing, they can also be used to quantify tracer losses (Fig. 3). All the same relationships hold if Ti and Zr are exported via colloids from a given sample of soil, rather than being gained (mixed). Both υ and m_C simply become negative, reflecting a loss of the tracer elements.

The formulation of the tracer ratio $R_{Ti/(Ti+Zr)}$ in Eq. (1), as opposed to a simple ratio, is required by the wide variations in the ratios of Ti to Zr. Depending on which element is in the numerator, values of υ would differ significantly when calculated using simple ratios of Ti/Zr versus Zr/Ti (Bern and Chadwick, 2010). In applications where the ratio in one component is 2× greater than the other, υ can differ by >17%. The Ti/Zr ratio we calculate for the colloids is almost 12× greater than for the granites and could cause υ to differ by >50%. Using values of $R_{Ti/(Ti+Zr)}$ from Eq. (1) as tracers eliminates this problem and yields identical υ values whether Ti or Zr is placed in the numerator (Bern and Chadwick, 2010).

Eq. (7) uses $R_{Ti/(Ti+Zr)}$ calculated from concentrations in samples and the parameter υ is dimensionless. To better assess the magnitude of colloid redistribution, results can be related to both tracer mass and overall soil horizon mass. Eq. (4) can be rearranged to show that the combined mass of Ti and Zr in a soil horizon is proportional (Fig. 4) to their masses in both redistributed colloids and parent material:

$$m_C = (m_C + m_{PM})^*\upsilon = m_S{}^*\upsilon. \tag{8}$$

This allows the mass of Ti and Zr in original parent material and redistributed colloidal material to be calculated for a given horizon.

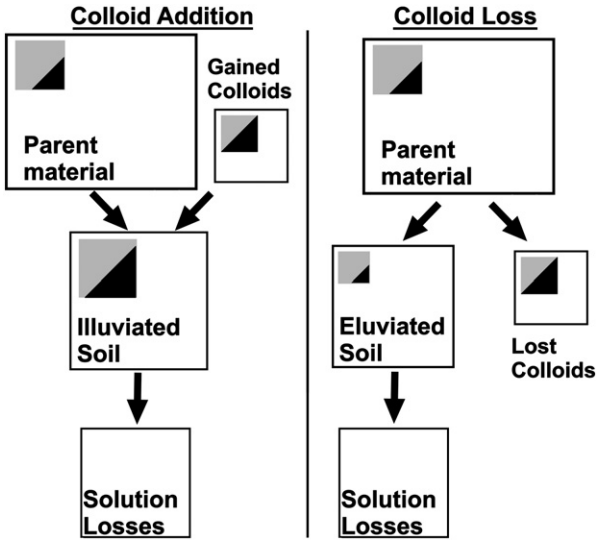

Fig. 4. Conceptual diagram of how the equations of the model are used to determine mass balance relationships. The black and gray squares represent the mass (m) of Ti and Zr in different components and the tracer ratio $R_{Ti/(Ti+Zr)}$ is represented by differences in black and gray shading, Bulk material mass (M) is represented by the surrounding squares. Material lost via solution is assumed to not contain Ti or Zr and has no shaded square. When colloids are added or mixed, as with illuviated soil (left panel), the total amount of tracer, its ratio, and quantity of bulk material change proportionally in the soil. When colloids are removed, as with eluviated soil (right panel), the total amount of tracer, its ratio, and quantity of bulk material change proportionally in the soil.

The concentrations of Ti and Zr in colloids (Ti_C and Zr_C respectively) can then be used to determine the total mass of colloidal material redistributed (M_C) by

$$M_C = \frac{m_C}{Ti_C + Zr_C}. \quad (9)$$

An identical calculation can be made for parent material. Knowing the mass of colloidal material redistributed for a horizon (M_C) allows the amount of a given element redistributed by colloids to be calculated, if the concentration of the element in colloidal material is known.

The bulk masses of soil (M_S), colloids (M_C) and parent material (M_{PM}) can all therefore be determined for a given horizon. If no processes other than colloidal redistribution were acting upon the soil horizon in question, then

$$M_S = M_{PM} + M_C. \quad (10)$$

However, soils are open systems that gain and lose elements in dissolved form and this invalidates Eq. (10). A better accounting of mass changes in soil incorporates mass gains or losses via dissolved elements (M_D) and takes the form

$$M_S = M_{PM} + M_C + M_D. \quad (11)$$

Eq. (11) is then easily rearranged to determine mass gains or losses via dissolved elements by

$$M_D = M_S - M_{PM} - M_C. \quad (12)$$

In this fashion, two distinct processes of mass transfer (in solution and in suspension) can be assessed in their influence in transforming parent material into soil (Fig. 4).

The validity of all data used in the calculations described above is crucial to the validity of the output, but the tracer ratios deserve particular consideration. Uncertainty regarding the $R_{Ti/(Ti+Zr)}$ of soil horizons could cause errors in individual determinations of υ, but uncertainty regarding the $R_{Ti/(Ti+Zr)}$ of colloids and parent material will generate systematic errors across the dataset. Colloidal $R_{Ti/(Ti+Zr)}$ is based on a single sample which makes assessment of variability at the study site impossible. Fortunately, that ratio is substantially different from soil or rock values and also relatively high (0.9928), thus the effect of uncertainty regarding colloidal $R_{Ti/(Ti+Zr)}$ on the calculations is proportionately small (Bern and Chadwick, 2010). For example, a 25% error in determining colloidal Ti or Zr concentration would cause a maximum error of 3% in the calculated extremes of colloidal illuviation or eluviation for this dataset. Thus even a potentially low recovery of Zr from digests of the colloid sample would generate proportionately little uncertainty.

In contrast, variability of $R_{Ti/(Ti+Zr)}$ determined for granite and C horizon samples is proportionately large and therefore the dominant source of uncertainty in calculating υ. Uncertainty regarding this parent material value has a large effect because it separates eluviation from illuviation, and the magnitude of its effect increases linearly with decreasing υ values (Bern and Chadwick, 2010). In subsequent figures and tables, the effect of parent material uncertainty is assessed by using the full range of $R_{Ti/(Ti+Zr)}$ calculated for the granite hand samples (0.8623–0.9234)(Fig. 3). The individual concentrations of Ti and Zr and their combined mass in parent material (m_{PM}) also strongly influence the output of calculations and the effect of these uncertainties are assessed using their ±1 S.D. values for granite.

4.3. Quantification results

Values of υ calculated using the mean $R_{Ti/(Ti+Zr)}$ of parent material range from −0.94 to 0.64 along the catena (Supplementary material). This corresponds to a maximum loss of 48% of the combined Ti and Zr tracer mass for one horizon and a gain of 175% for another. Losses of bulk colloidal material compared to calculated bulk parent material are high in the strongly redox-influenced seepline, where colloidal mobilization might be expected to be greatest (Thompson et al., 2006). There, colloidal transfers have removed up to 6% of the original mass of several B horizons in seepline profile 5 and 6 (Fig 5). Colloidal losses integrated over seepline profiles 5 and 6 are 110 and 106 kg m^{-2}, respectively (Fig 6). The similarly great 94 kg m^{-2} colloidal loss from profile 1 may be due to lack of upslope-derived, illuvial inputs. Colloidal gains are a notable feature in portions of the downslope soil profiles, particularly one B horizon in profile 9, which has gained 22% colloidal mass relative to parent material. Overall, profile 9 has gained 169 kg m^{-2} of colloidal material, an increase of 10% relative to parent material. Profile depths and bulk densities were comparable for all volumetric comparisons (Supplementary material).

Solution losses are greatest at the seepline and uppermost downslope profile, where water from upslope passes through the soil matrix before being forced to the surface. In fact, several horizons have lost >50% of parent material mass (Fig. 5). Profiles 5 and 6 have lost 1199, and 1418 kg m^{-2} of material via solution, respectively, 11–13× more mass than lost via colloids (Fig. 6). Profile 1, which receives no compensating additions from upslope, has lost 1273 kg m^{-2} of material via solution, and losses diminish in profiles immediately downslope. Similar to seepline profiles 5 and 6, solutional losses at the crest of the catena are 13× greater than colloidal losses. Downslope profile 7 has incurred solutional losses similar to seepline, but further downslope those losses are much smaller and range from 195 to 403 kg m^{-2}. Such small solutional losses speak to the reduced flow of water through these clay-rich profiles. No soil horizon shows definitive gains of material carried by solution, which suggests that authigenic mineral formation from elements in solution is not a significant process in these soils.

The model presented here is not meant to replace the tau and similar calculations used for determining element mobility during weathering using HFS elements like Zr as an index element (Brimhall and Dietrich, 1987; Muir and Logan, 1982) However, our model has implications for weathering calculations in settings where colloidal

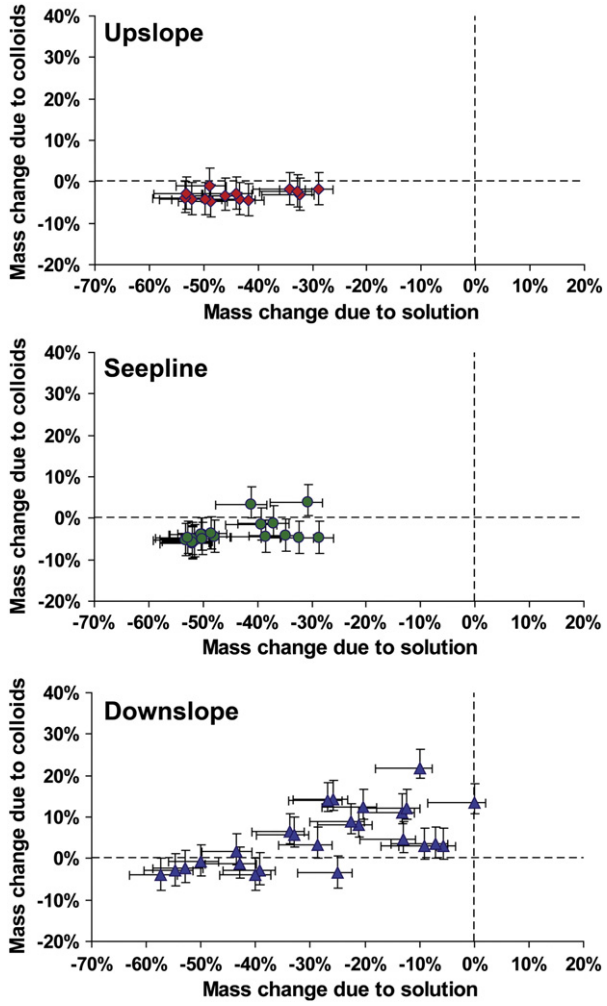

Fig. 5. Percentage mass loss (−) or gain (+) via suspended solids (colloids) and solution for the <2 mm fraction of individual soil horizons. Error bars depict the range of uncertainty using the ±1 S.D. concentrations of Ti and Zr to calculate soil parent material $R_{Ti/(Ti+Zr)}$. Dashed lines separate mass loss and gain for each axis.

transport of HFS elements is an important process. Table 2 shows gains and losses of Ti and Zr from soil profiles as percentages relative to parent material. Colloidal losses of Zr reach 3% in parts of the catena, and gains reach 6% downslope. Without accounting for colloidal Zr transfers, tau values would underestimate weathering upslope on the catena and overestimate it downslope. Redistributions of Ti are truly significant, ranging from a 41% loss from profile 5 to a 90% gain in profile 9. Any assessment of weathering of these soils that

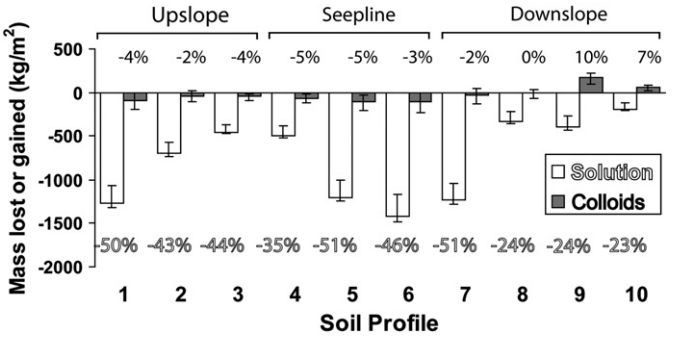

Fig. 6. Calculated mass loss (−) or gain (+) summed for profiles via suspended solids (colloids) and solution. Error bars depict the range of uncertainty associated with soil parent material composition as described in the text. Percentages show gains and losses relative to parent material and account for difference in profile depth.

Table 2
Gains and losses of Zr and Ti for soil profiles along the catena calculated using the mean concentrations and $R_{Ti/(Ti+Zr)}$ of parent material (PM) and ranges based upon uncertainty estimates described in the text.

Profile	Zr redistribution by colloids		Ti redistribution by colloids	
	PM mean	PM range	PM mean	PM range
1	−2%	−4% to 0%	−33%	−48% to 5%
2	−1%	−3% to 1%	−21%	−39% to 23%
3	−3%	−4% to 0%	−39%	−54% to −5%
4	−3%	−4% to 0%	−40%	−54% to −7%
5	−3%	−4% to 0%	−41%	−55% to −8%
6	−2%	−3% to 0%	−31%	−47% to 8%
7	−1%	−2% to 2%	−13%	−33% to 34%
8	0%	−2% to 3%	−4%	−26% to 48%
9	6%	4% to 12%	90%	48% to 191%
10	4%	2% to 9%	59%	24% to 145%

was indexed to Ti would therefore suffer major errors. Evidence that Ti and Zr are mobile in soils is not new (e.g. Colin et al., 1993; Cornu et al., 1999). The novelty of the model presented here is that it determines mobility in a quantitative fashion that acknowledges both elements as mobile, rather than qualitatively comparing elements to determine which is least mobile.

5. Conclusions

Comparisons of concentration ratios of the high field strength elements Ti and Zr in colloids, soil, and parent material of a granitic catena show that those elements are differentially redistributed by colloidal transport in a manner that supports the traditional understanding of catena eluvial and illuvial zones. Using the model presented, the ratio $R_{Ti/(Ti+Zr)}$ can be employed as a robust, quantitative tracer of colloid redistribution in this setting, and solutional transfers can be obtained by difference from total change in soil mass relative to parent material mass. Despite considerable uncertainty in the chemical composition of the soil parent material, the resulting patterns of mass redistribution are greater than the uncertainty in the calculations. Along this catena, colloidal mass losses are smaller than solution losses; soil mass gains via colloids generally occur within horizons that have experienced smaller, but still substantial solution losses. The mobility and redistribution of Ti and Zr documented here serves as yet another caution to using them as immobile index elements for weathering calculations. However, the ability to quantify such redistributions offers the potential to correct for redistribution effects.

Supplementary materials related to this article can be found online at doi:10.1016/j.chemgeo.2011.01.014

Acknowledgements

This work was supported by the Andrew W. Mellon Foundation. We thank the Kruger National Park scientific support staff and game guards for logistical support and Mary Kay Amistadi, Paul Lamothe, Katie Lindeburg, Heather Lowers and Frank Setaro for laboratory support. Dan Muhs, Rich Reynolds and two anonymous reviewers provided comments that improved this paper.

References

Barton Jr., J.H., Bristow, J.W., Venter, F.J., 1986. A summary of the Precambrian granitoid rocks of the Kruger National Park. Koedoe 29, 39–44.
Bern, C.R., Chadwick, O.A., 2010. Quantifying colloid mass redistribution in soils and other physical mass transfers. In: Birkle, P., Torres-Alvarado, I.S. (Eds.), Water Rock Interaction. CRC Press, Taylor & Francis Group, New York, pp. 765–768.
Blake, G.R., Hartge, K.H., 1986. Bulk density. In: Klute, A. (Ed.), Methods of Soil Analysis. ASA and SSSA, Madison, WI, pp. 363–375.
Brewer, R., 1964. Fabric and Mineral Analysis of Soils. John Wiley, New York. 470 pp.
Brimhall, G.H., Dietrich, W.E., 1987. Constitutive mass balance relations between chemical composition, volume, density, porosity, and strain in metasomatic

hydrochemical systems: results on weathering and pedogenesis. Geochimica et Cosmochimica Acta 51 (3), 567–587.
Bunn, R.A., Magelkey, R.D., Ryan, J.N., Elimelech, M., 2002. Mobilization of natural colloids from an iron oxide-coated sand aquifer: effect of pH and ionic strength. Environmental Science & Technology 36, 314–322.
Colin, F., Alarçon, C., Vieillard, P., 1993. Zircon: an immobile index in soils? Chemical Geology 107, 273–276.
Cornu, S., et al., 1999. Evidence of titanium mobility in soil profiles, Manaus, central Amazonia. Geoderma 91, 281–295.
EPA, U.S., 1986. SW-846, Test Methods for Evaluating Solid Waste, Method 3502. US GPO, Washington D.C.
Faure, G., 1977. Principles of Isotope Geology. John Wiley & Sons, New York.
Gasser, U.G., Juchler, S.J., Sticher, H., 1994. Chemistry and speciation of soil water from serpantinitic soils: importance of colloids in the transport of Cr, Fe, Mg, and Ni. Soil Science 158, 314–322.
Gee, G.W., Bauder, J.W., 1986. Particle-size analysis. In: Klute, A. (Ed.), Methods of Soil Analysis, Part 1. Physical and Mineralogical Methods. American Society of Agronomy — Soil Science Society of America, Madison, Wisconsin.
Heil, D., Sposito, G., 1993. Organic-matter role in illitic soil colloids flocculation: I. Counter ions and pH. Soil Science Society of America Journal 57, 1241–1246.
Huggett, R.J., 1975. Soil landscape systems: a model of soil genesis. Geoderma 13 (1), 1–22.
Jenny, H., Smith, G.D., 1935. Colloid chemical aspects of clay pan formation in soil profiles. Soil Science 39, 377–379.
Khomo, L.M., 2008. Weathering and soil properties on old granitic catenas along climo-topographic gradients in Kruger National Park, University of the Witwatersrand, Johannesburg, PhD Thesis, 232 pp.
Kretzschmar, R., Borkovec, M., Grolimund, D., Elimelech, M., 1999. Mobile subsurface colloids and their role in contaminant transport. Advances in Agronomy 66, 121–193.
Kurtz, A.C., Derry, L.A., Chadwick, O.A., Alfano, M.J., 2000. Refractory element mobility in volcanic soils. Geology 28 (8), 683–686.
Laegdsmand, M., Villholth, K.G., Ullum, M., Jensen, K.H., 1999. Processes of colloid mobilization and transport in macroporous soil monoliths. Geoderma 93, 33–59.
McCarthy, J.F., McKay, L.D., 2004. Colloid transport in the subsurface: past, present, and future challenges. Vadose Zone Journal 3, 326–337.
Muir, J.W., Logan, J., 1982. Eluvial/illuvial coefficients of major elements and the corresponding loses and gains in three soil profiles. Journal of Soil Science 33, 295–308.
Parkhurst, D.L., Appelo, C.A.J., 1999. User's guide to PHREEQC (Version 2) — a computer program for speciation, batch-reaction, one-dimensional transport, and inverse geochemical calculations. U.S. Geological Survey Water-Resources Investigations Report 99–4259. 310 pp.
Paton, T.R., Humphreys, G.S., Mitchell, P.B., 1995. Soils: A New Global View. UCL Press, London. 213 pp.
Ryan, J.N., Illangaskare, T.H., Litaor, M.I., Shannon, R., 1998. Particle and plutonium mobilization in macroporous soils during rainfall simulations. Environmental Science & Technology 32 (476–482).
Scholes, R.J., et al., 2001. The environment and vegetation of the flux measurement site near Skukuza, Kruger National Park. Koedoe 44 (1), 73–83.
Sommer, M., Schlichting, E., 1997. Archetypes of catenas in respect to matter — a concept for structuring and grouping catenas. Geoderma 76, 1–33.
Sommer, M., Halm, D., Weller, U., Zarei, M., Stahr, K., 2000. Lateral podzolization in a granite landscape. Soil Science Society of America Journal 64, 1434–1442.
Suarez, D.L., Rhodes, J.D., Lavado, R., Grieve, C.M., 1984. Effect of pH on saturated hydraulic conductivity and soil dispersion. Soil Science Society of America Journal 48, 50–55.
Thompson, A., Chadwick, O.A., Boman, S., Chorover, J., 2006. Colloid mobilization during soil iron redox oscillations. Environmental Science & Technology 40, 5743–5749.
Venter, F.J., 1986. Soil patterns associated with the major geological units of the Kruger National Park. Koedoe 29, 125–138.
Walker, P.H., Chittleborough, D.J., 1986. Development of particle-size distributions in some alfisols of southeastern Australia. Soil Science Society of America Journal 50 (394–400).